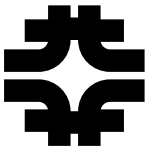

# Fermi National Accelerator Laboratory

**FERMILAB-Pub-98/252-E**
**CDF**

# Search for Higgs Bosons Produced in Association with a Vector Boson in $p\bar{p}$ Collisions at $\sqrt{s}$ = 1.8 TeV

F. Abe et al.
The CDF Collaboration

*Fermi National Accelerator Laboratory*
*P.O. Box 500, Batavia, Illinois 60510*

September 1998

Submitted to *Physical Review Letters*

Operated by Universities Research Association Inc. under Contract No. DE-AC02-76CH03000 with the United States Department of Energy

## Disclaimer



## Distribution



## Copyright Notification

# Search for Higgs Bosons Produced in Association with a Vector Boson in $p\bar{p}$ Collisions at $\sqrt{s} = 1.8$ TeV

F. Abe,[17] H. Akimoto,[39] A. Akopian,[31] M. G. Albrow,[7] A. Amadon,[5] S. R. Amendolia,[27] D. Amidei,[20] J. Antos,[33] S. Aota,[37] G. Apollinari,[31] T. Arisawa,[39] T. Asakawa,[37] W. Ashmanskas,[18] M. Atac,[7] P. Azzi-Bacchetta,[25] N. Bacchetta,[25] S. Bagdasarov,[31] M. W. Bailey,[22] P. de Barbaro,[30] A. Barbaro-Galtieri,[18] V. E. Barnes,[29] B. A. Barnett,[15] M. Barone,[9] G. Bauer,[19] T. Baumann,[11] F. Bedeschi,[27] S. Behrends,[3] S. Belforte,[27] G. Bellettini,[27] J. Bellinger,[40] D. Benjamin,[35] J. Bensinger,[3] A. Beretvas,[7] J. P. Berge,[7] J. Berryhill,[5] S. Bertolucci,[9] S. Bettelli,[27] B. Bevensee,[26] A. Bhatti,[31] K. Biery,[7] C. Bigongiari,[27] M. Binkley,[7] D. Bisello,[25] R. E. Blair,[1] C. Blocker,[3] K. Bloom,[15] S. Blusk,[30] A. Bodek,[30] W. Bokhari,[26] G. Bolla,[29] Y. Bonushkin,[4] D. Bortoletto,[29] J. Boudreau,[28] L. Breccia,[2] C. Bromberg,[21] N. Bruner,[22] R. Brunetti,[2] E. Buckley-Geer,[7] H. S. Budd,[30] K. Burkett,[11] G. Busetto,[25] A. Byon-Wagner,[7] K. L. Byrum,[1] M. Campbell,[20] A. Caner,[27] W. Carithers,[18] D. Carlsmith,[40] J. Cassada,[30] A. Castro,[25] D. Cauz,[36] A. Cerri,[27] P. S. Chang,[33] P. T. Chang,[33] H. Y. Chao,[33] J. Chapman,[20] M. -T. Cheng,[33] M. Chertok,[34] G. Chiarelli,[27] C. N. Chiou,[33] F. Chlebana,[7] L. Christofek,[13] M. L. Chu,[33] S. Cihangir,[7] A. G. Clark,[10] M. Cobal,[27] E. Cocca,[27] M. Contreras,[5] J. Conway,[32] J. Cooper,[7] M. Cordelli,[9] D. Costanzo,[27] C. Couyoumtzelis,[10] D. Cronin-Hennessy,[6] R. Culbertson,[5] D. Dagenhart,[38] T. Daniels,[19] F. DeJongh,[7] S. Dell'Agnello,[9] M. Dell'Orso,[27] R. Demina,[7] L. Demortier,[31] M. Deninno,[2] P. F. Derwent,[7] T. Devlin,[32] J. R. Dittmann,[6] S. Donati,[27] J. Done,[34] T. Dorigo,[25] N. Eddy,[13] K. Einsweiler,[18] J. E. Elias,[7] R. Ely,[18] E. Engels, Jr.,[28] W. Erdmann,[7] D. Errede,[13] S. Errede,[13] Q. Fan,[30] R. G. Feild,[41] Z. Feng,[15] C. Ferretti,[27] I. Fiori,[2] B. Flaugher,[7] G. W. Foster,[7] M. Franklin,[11] J. Freeman,[7] J. Friedman,[19] H. Frisch,[5] Y. Fukui,[17] S. Gadomski,[14] S. Galeotti,[27] M. Gallinaro,[26]

O. Ganel,[35] M. Garcia-Sciveres,[18] A. F. Garfinkel,[29] C. Gay,[41] S. Geer,[7] D. W. Gerdes,[15] P. Giannetti,[27] N. Giokaris,[31] P. Giromini,[9] G. Giusti,[27] M. Gold,[22] A. Gordon,[11] A. T. Goshaw,[6] Y. Gotra,[28] K. Goulianos,[31] H. Grassmann,[36] L. Groer,[32] C. Grosso-Pilcher,[5] G. Guillian,[20] J. Guimaraes da Costa,[15] R. S. Guo,[33] C. Haber,[18] E. Hafen,[19] S. R. Hahn,[7] R. Hamilton,[11] T. Handa,[12] R. Handler,[40] F. Happacher,[9] K. Hara,[37] A. D. Hardman,[29] R. M. Harris,[7] F. Hartmann,[16] J. Hauser,[4] E. Hayashi,[37] J. Heinrich,[26] W. Hao,[35] B. Hinrichsen,[14] K. D. Hoffman,[29] M. Hohlmann,[5] C. Holck,[26] R. Hollebeek,[26] L. Holloway,[13] Z. Huang,[20] B. T. Huffman,[28] R. Hughes,[23] J. Huston,[21] J. Huth,[11] H. Ikeda,[37] M. Incagli,[27] J. Incandela,[7] G. Introzzi,[27] J. Iwai,[39] Y. Iwata,[12] E. James,[20] H. Jensen,[7] U. Joshi,[7] E. Kajfasz,[25] H. Kambara,[10] T. Kamon,[34] T. Kaneko,[37] K. Karr,[38] H. Kasha,[41] Y. Kato,[24] T. A. Keaffaber,[29] K. Kelley,[19] R. D. Kennedy,[7] R. Kephart,[7] D. Kestenbaum,[11] D. Khazins,[6] T. Kikuchi,[37] B. J. Kim,[27] H. S. Kim,[14] S. H. Kim,[37] Y. K. Kim,[18] L. Kirsch,[3] S. Klimenko,[8] D. Knoblauch,[16] P. Koehn,[23] A. Köngeter,[16] K. Kondo,[37] J. Konigsberg,[8] K. Kordas,[14] A. Korytov,[8] E. Kovacs,[1] W. Kowald,[6] J. Kroll,[26] M. Kruse,[30] S. E. Kuhlmann,[1] E. Kuns,[32] K. Kurino,[12] T. Kuwabara,[37] A. T. Laasanen,[29] S. Lami,[27] S. Lammel,[7] J. I. Lamoureux,[3] M. Lancaster,[18] M. Lanzoni,[27] G. Latino,[27] T. LeCompte,[1] S. Leone,[27] J. D. Lewis,[7] M. Lindgren,[4] T. M. Liss,[13] J. B. Liu,[30] Y. C. Liu,[33] N. Lockyer,[26] O. Long,[26] C. Loomis,[32] M. Loreti,[25] D. Lucchesi,[27] P. Lukens,[7] S. Lusin,[40] J. Lys,[18] K. Maeshima,[7] P. Maksimovic,[11] M. Mangano,[27] M. Mariotti,[25] J. P. Marriner,[7] G. Martignon,[25] A. Martin,[41] J. A. J. Matthews,[22] P. Mazzanti,[2] K. McFarland,[30] P. McIntyre,[34] P. Melese,[31] M. Menguzzato,[25] A. Menzione,[27] E. Meschi,[27] S. Metzler,[26] C. Miao,[20] T. Miao,[7] G. Michail,[11] R. Miller,[21] H. Minato,[37] S. Miscetti,[9] M. Mishina,[17] S. Miyashita,[37] N. Moggi,[27] E. Moore,[22] Y. Morita,[17] A. Mukherjee,[7] T. Muller,[16] P. Murat,[27] S. Murgia,[21] M. Musy,[36] H. Nakada,[37] T. Nakaya,[5] I. Nakano,[12] C. Nelson,[7] D. Neuberger,[16] C. Newman-Holmes,[7] C.-Y. P. Ngan,[19] L. Nodulman,[1] A. Nomerotski,[8] S. H. Oh,[6] T. Ohmoto,[12] T. Ohsugi,[12] R. Oishi,[37] M. Okabe,[37] T. Okusawa,[24] J. Olsen,[40] C. Pagliarone,[27] R. Paoletti,[27] V. Papadimitriou,[35] S. P. Pappas,[41] N. Parashar,[27] A. Parri,[9] J. Patrick,[7] G. Pauletta,[36] M. Paulini,[18] A. Perazzo,[27] L. Pescara,[25] M. D. Peters,[18]

T. J. Phillips,[6] G. Piacentino,[27] M. Pillai,[30] K. T. Pitts,[7] R. Plunkett,[7] A. Pompos,[29] L. Pondrom,[40] J. Proudfoot,[1] F. Ptohos,[11] G. Punzi,[27] K. Ragan,[14] D. Reher,[18] M. Reischl,[16] A. Ribon,[25] F. Rimondi,[2] L. Ristori,[27] W. J. Robertson,[6] T. Rodrigo,[27] S. Rolli,[38] L. Rosenson,[19] R. Roser,[13] T. Saab,[14] W. K. Sakumoto,[30] D. Saltzberg,[4] A. Sansoni,[9] L. Santi,[36] H. Sato,[37] P. Schlabach,[7] E. E. Schmidt,[7] M. P. Schmidt,[41] A. Scott,[4] A. Scribano,[27] S. Segler,[7] S. Seidel,[22] Y. Seiya,[37] F. Semeria,[2] T. Shah,[19] M. D. Shapiro,[18] N. M. Shaw,[29] P. F. Shepard,[28] T. Shibayama,[37] M. Shimojima,[37] M. Shochet,[5] J. Siegrist,[18] A. Sill,[35] P. Sinervo,[14] P. Singh,[13] K. Sliwa,[38] C. Smith,[15] F. D. Snider,[15] J. Spalding,[7] T. Speer,[10] P. Sphicas,[19] F. Spinella,[27] M. Spiropulu,[11] L. Spiegel,[7] L. Stanco,[25] J. Steele,[40] A. Stefanini,[27] R. Ströhmer,[7a] J. Strologas,[13] F. Strumia, [10] D. Stuart,[7] K. Sumorok,[19] J. Suzuki,[37] T. Suzuki,[37] T. Takahashi,[24] T. Takano,[24] R. Takashima,[12] K. Takikawa,[37] M. Tanaka,[37] B. Tannenbaum,[22] F. Tartarelli,[27] W. Taylor,[14] M. Tecchio,[20] P. K. Teng,[33] Y. Teramoto,[24] K. Terashi,[37] S. Tether,[19] D. Theriot,[7] T. L. Thomas,[22] R. Thurman-Keup,[1] M. Timko,[38] P. Tipton,[30] A. Titov,[31] S. Tkaczyk,[7] D. Toback,[5] K. Tollefson,[30] A. Tollestrup,[7] H. Toyoda,[24] W. Trischuk,[14] J. F. de Troconiz,[11] S. Truitt,[20] J. Tseng,[19] N. Turini,[27] T. Uchida,[37] F. Ukegawa,[26] J. Valls,[32] S. C. van den Brink,[28] S. Vejcik, III,[20] G. Velev,[27] R. Vidal,[7] R. Vilar,[7a] D. Vucinic,[19] R. G. Wagner,[1] R. L. Wagner,[7] J. Wahl,[5] N. B. Wallace,[27] A. M. Walsh,[32] C. Wang,[6] C. H. Wang,[33] M. J. Wang,[33] A. Warburton,[14] T. Watanabe,[37] T. Watts,[32] R. Webb,[34] C. Wei,[6] H. Wenzel,[16] W. C. Wester, III,[7] A. B. Wicklund,[1] E. Wicklund,[7] R. Wilkinson,[26] H. H. Williams,[26] P. Wilson,[7] B. L. Winer,[23] D. Winn,[20] D. Wolinski,[20] J. Wolinski,[21] S. Worm,[22] X. Wu,[10] J. Wyss,[27] A. Yagil,[7] W. Yao,[18] K. Yasuoka,[37] G. P. Yeh,[7] P. Yeh,[33] J. Yoh,[7] C. Yosef,[21] T. Yoshida,[24] I. Yu,[7] A. Zanetti,[36] F. Zetti,[27] and S. Zucchelli[2]

(CDF Collaboration)

[1] *Argonne National Laboratory, Argonne, Illinois 60439*

[2] *Istituto Nazionale di Fisica Nucleare, University of Bologna, I-40127 Bologna, Italy*

[3] *Brandeis University, Waltham, Massachusetts 02254*

[4] *University of California at Los Angeles, Los Angeles, California 90024*

[5] *University of Chicago, Chicago, Illinois 60637*

[6] *Duke University, Durham, North Carolina 27708*

[7] *Fermi National Accelerator Laboratory, Batavia, Illinois 60510*

[8] *University of Florida, Gainesville, Florida 32611*

[9] *Laboratori Nazionali di Frascati, Istituto Nazionale di Fisica Nucleare, I-00044 Frascati, Italy*

[10] *University of Geneva, CH-1211 Geneva 4, Switzerland*

[11] *Harvard University, Cambridge, Massachusetts 02138*

[12] *Hiroshima University, Higashi-Hiroshima 724, Japan*

[13] *University of Illinois, Urbana, Illinois 61801*

[14] *Institute of Particle Physics, McGill University, Montreal H3A 2T8, and University of Toronto, Toronto M5S 1A7, Canada*

[15] *The Johns Hopkins University, Baltimore, Maryland 21218*

[16] *Institut für Experimentelle Kernphysik, Universität Karlsruhe, 76128 Karlsruhe, Germany*

[17] *National Laboratory for High Energy Physics (KEK), Tsukuba, Ibaraki 305, Japan*

[18] *Ernest Orlando Lawrence Berkeley National Laboratory, Berkeley, California 94720*

[19] *Massachusetts Institute of Technology, Cambridge, Massachusetts 02139*

[20] *University of Michigan, Ann Arbor, Michigan 48109*

[21] *Michigan State University, East Lansing, Michigan 48824*

[22] *University of New Mexico, Albuquerque, New Mexico 87131*

[23] *The Ohio State University, Columbus, Ohio 43210*

[24] *Osaka City University, Osaka 588, Japan*

[25] *Universita di Padova, Istituto Nazionale di Fisica Nucleare, Sezione di Padova, I-35131 Padova, Italy*

[26] *University of Pennsylvania, Philadelphia, Pennsylvania 19104*

[27] *Istituto Nazionale di Fisica Nucleare, University and Scuola Normale Superiore of Pisa, I-56100 Pisa, Italy*

[28] *University of Pittsburgh, Pittsburgh, Pennsylvania 15260*

[29] *Purdue University, West Lafayette, Indiana 47907*

[30] *University of Rochester, Rochester, New York 14627*

[31] *Rockefeller University, New York, New York 10021*

[32] *Rutgers University, Piscataway, New Jersey 08855*

[33] *Academia Sinica, Taipei, Taiwan 11530, Republic of China*

[34] *Texas A&M University, College Station, Texas 77843*

[35] *Texas Tech University, Lubbock, Texas 79409*

[36] *Istituto Nazionale di Fisica Nucleare, University of Trieste/ Udine, Italy*

[37] *University of Tsukuba, Tsukuba, Ibaraki 315, Japan*

[38] *Tufts University, Medford, Massachusetts 02155*

[39] *Waseda University, Tokyo 169, Japan*

[40] *University of Wisconsin, Madison, Wisconsin 53706*

[41] *Yale University, New Haven, Connecticut 06520*

## Abstract

We search for Higgs bosons produced in association with a massive vector boson in $91 \pm 7$ pb$^{-1}$ of $p\bar{p}$ collisions at $\sqrt{s} = 1.8$ TeV recorded by the Collider Detector at Fermilab. We assume the Higgs scalar $H^0$ decays to a $b\bar{b}$ pair with branching ratio $\beta$, and we consider the hadronic decays of the vector boson $V$ ($W$ or $Z$). Observations are consistent with background expectations. We place 95% confidence level upper limits on $\sigma(p\bar{p} \to H^0 V) \cdot \beta$ as a function of the scalar mass ($M_{H^0}$) over the range 70 GeV/$c^2$ $< M_{H^0} <$ 140 GeV/$c^2$. When combined with an analysis of the case where $V$ is a leptonically decaying $W$, these limits vary from 23 pb at $M_{H^0} = 70$ GeV/$c^2$ to 17 pb at $M_{H^0} = 140$ GeV/$c^2$.

One of the primary goals of present and future colliders is to reveal the mechanism responsible for the symmetry breaking of the electroweak interaction. The simplest model for this mechanism is spontaneous symmetry breaking achieved through the introduction of a scalar field doublet [1]. This leaves a single observable scalar particle, the Higgs boson, with unknown mass but fixed couplings to other particles. The possible range for the mass extends from a lower bound of 77.5 GeV/$c^2$ from the LEP experiments [2] to $\mathcal{O}(1)$ TeV. Precision electroweak experiments suggest that the Higgs boson mass may lie at the lower end of this range [3]. The dominant decay mode of the Higgs boson up to $M_{H^0} \sim 130$ GeV/$c^2$ is $H^0 \to b\bar{b}$. A similar symmetry breaking mechanism occurs in the minimal supersymmetric extension of the standard model, where several observable scalar states are predicted, the lightest of which is expected to have a mass below 135 GeV/$c^2$ [4].

In $p\bar{p}$ collisions, the Higgs production mechanism with the most promising detection possibilities is $p\bar{p} \to V + H^0$, where $V = W, Z$. In the framework of the standard model, the production cross section in this channel is 1.3 to 0.11 pb for Higgs masses between 70 to 140 GeV/$c^2$ [5]. This is out of the scope of the present analysis, using $91 \pm 7$ pb$^{-1}$ of $p\bar{p}$ collisions at $\sqrt{s} = 1.8$ TeV recorded by the Collider Detector at Fermilab (CDF). In this letter we therefore report on a search for a Higgs scalar produced in association with a vector boson ($p\bar{p} \to V + H^0$, where $V = W, Z$) with unknown cross section $\sigma_{VH^0}$. We look for $H^0$ decays to a $b\bar{b}$ pair with unknown branching ratio $\beta$, and for hadronic decays of the vector boson ($W \to q\bar{q}'$, $Z \to q\bar{q}$). The experimental signature considered is four jets in the final state, with two of them identified as $b$ jets. The CDF [6] and D0 [7] collaborations recently reported on direct searches for $W + H^0$ where the $W$ was identified by its decay to $e\nu$ or $\mu\nu$. The all-hadronic channel described here has the advantage of a larger branching ratio, but suffers from a larger QCD background. Finally, we combine the limits obtained in the all-hadronic channel with those from our previous search for $W + H^0$.

The CDF detector has been described in detail elsewhere [8]. The CDF silicon vertex detector (SVX) consists of four layers of axial microstrips located immediately outside the

beampipe with an innermost radius of 2.9 cm [9]. The SVX provides precise track reconstruction in the plane transverse to the beam and the ability to identify secondary vertices produced by heavy flavor decays. The momenta of charged particles are measured in the central tracking chamber (CTC), which is inside a 1.4 T axial magnetic field. Outside the CTC, electromagnetic and hadronic calorimeters arranged in a projective tower geometry cover the pseudorapidity region $|\eta| < 4.2$ [10] and are used to identify jets. The data sample was recorded with a trigger which requires four or more clusters of contiguous calorimeter towers, each with transverse energy $E_T \geq 15$ GeV, and a total transverse energy $\sum E_T \geq 125$ GeV.

The data reduction starts with a background filter to reject cosmic ray events, beam halo and detector noise. Events are required to have missing $E_T$ [10] significance $S \equiv \not\!\!E_T / (\sum E_T)^{1/2} < 6$ GeV$^{1/2}$, total energy less than 2000 GeV and a primary vertex reconstructed within 60 cm of the detector center. Events with isolated high-$E_T$ ($p_T$) electrons (muons), defined as in [6] are also removed. After this selection, events are required to have four or more jets with uncorrected $E_T > 15$ GeV and $|\eta| < 2.1$. Jets are defined as localized energy depositions in the calorimeters and are reconstructed using an iterative clustering algorithm with a fixed cone of radius $\Delta R = \sqrt{\Delta\eta^2 + \Delta\phi^2} = 0.4$ in $\eta - \phi$ space [11]. Jet energies are then corrected for energy losses in uninstrumented detector regions, energy falling outside the clustering cone, contributions from underlying event and multiple interactions, and calorimeter nonlinearities. After this initial selection the sample contains 207,604 events. In addition, we require that at least two among the four highest-$E_T$ jets in the event are identified (tagged) as $b$ quark candidates. We use the secondary vertex algorithm developed for the top quark observation [12]. The algorithm begins by searching for secondary vertices that contain three or more displaced tracks. If none are found, the algorithm searches for two-track vertices using more stringent track criteria. A jet is tagged if the secondary vertex transverse displacement from the primary one exceeds three times its uncertainty.

There are 764 events with four or more jets and two or more $b$-tags. In these

events, only the four highest-$E_T$ jets are considered for the mass reconstruction: the two highest-$E_T$ $b$-tagged jets are assigned to the Higgs boson, and the other two to the vector boson. The invariant mass of the $b$-tagged dijet system is defined as $M_{b\bar{b}} = \sqrt{2E_T^b E_T^{\bar{b}}[\cosh(\Delta\eta)_{b\bar{b}} - \cos(\Delta\phi)_{b\bar{b}}]}$. The $b\bar{b}$ invariant mass distribution in signal events, generated with the PYTHIA v5.6 Monte Carlo generator [13] together with a detector and trigger simulation, contains a Gaussian core with a sigma of $\sim 0.14 \times M_{H^0}$. The tails of the distribution are dominated by the cases (25-30%) where the jet assignment in the mass reconstruction is incorrect. In most of these cases, one of the jets assigned to the Higgs is a heavy quark jet from the decay of the $V$ boson [14].

The main source of background events is QCD heavy flavor production. The heavy flavor content of QCD hard processes has been modelled with the PYTHIA Monte Carlo program. We generated all QCD jet production channels and retained the events that contained a heavy quark produced either in the hard scattering or in the associated radiation process. Events with a heavy quark are conventionally classified in three groups: direct production, gluon splitting, and flavor excitation. Direct production events are characterized by a high value of the invariant mass, $M_{b\bar{b}}$, and a low value of the transverse momentum of the $b\bar{b}$ system, $p_T(b\bar{b})$. The same is true for flavor excitation events. The kinematics of final state gluon splitting events favor a relatively smaller invariant mass value and a large $p_T(b\bar{b})$, since both jets tend to be emitted along the same direction. Figure 1 shows $M_{b\bar{b}}$ versus $p_T(b\bar{b})$ for data, QCD $b\bar{b}/c\bar{c}$ Monte Carlo, and $V + H^0$ signal. In this plane, the Higgs signal shows a greater tendency to large $M_{b\bar{b}}$ and $p_T(b\bar{b})$ values. A cut on $p_T(b\bar{b}) \geq 50$ GeV/$c$ is $\sim 80\%$ efficient for the signal and strongly discriminates against direct production and flavor excitation of heavy quarks. After the $p_T(b\bar{b})$ requirement is applied to the data 589 events remain.

Other backgrounds are $t\bar{t}$ production, $Z$ + jets events with $Z \to b\bar{b}/c\bar{c}$ and fake double-tags. The first two are estimated from Monte Carlo and the last one from data. Using the CDF measured $t\bar{t}$ production cross section ($\sigma_{t\bar{t}} = 7.6^{+1.8}_{-1.5}$ pb) [15] and a top quark mass of

$M_t = 175$ GeV/$c^2$, the HERWIG v5.6 Monte Carlo generator [16] predicts $26 \pm 7$ $t\bar{t}$ events in the data, after trigger, kinematic and $b$-tag requirements. The same generator predicts $17 \pm 4$ $Z$ + jets background events. Fake double-tags are defined as events in which at least one of the two tagged jets contains a false secondary vertex in a light quark or gluon jet. Fake tag probabilities are parameterized by measuring in several inclusive jet data samples the proportion of jets in which a secondary vertex is reconstructed on the wrong side of the primary vertex with respect to the jet direction [12,17]. The current data set is estimated to contain $89 \pm 11$ fake double-tag events. Finally, other minor sources of background include $Wb\bar{b}/Wc\bar{c}$, $Zb\bar{b}/Zc\bar{c}$, diboson and single top production, and are estimated from Monte Carlo calculations. Together, they account for less than 1% of the total number of events, have a broad invariant mass distribution, and are neglected in the final fit.

The total signal detection efficiency is defined as the product of the trigger efficiency, the kinematical and geometrical acceptances, the double $b$-tagging efficiency, the $p_T(b\bar{b})$ cut efficiency, and the branching fraction $\mathcal{B}(W \to q\bar{q}') = 67.9 \pm 1.5\%$ or $\mathcal{B}(Z \to q\bar{q}) = 69.90 \pm 0.15\%$ [18,3]. The combined trigger and acceptance efficiency is determined using PYTHIA followed by detector and trigger simulations. The QQ v9.1 [19] Monte Carlo generator is used to model the decays of the $b$ hadrons. The combined trigger and acceptance efficiency depends on the Higgs mass and increases from $8 \pm 1\%$ for $M_{H^0} = 70$ GeV/$c^2$ to $31 \pm 3\%$ for $M_{H^0} = 140$ GeV/$c^2$ [14]. The uncertainty is dominated by the systematics related to QCD radiation modelling. The SVX double $b$-tagging efficiency is calculated with a combination of data and Monte Carlo samples and is $14 \pm 3\%$ with a small dependence on the Higgs mass. The total efficiency increases linearly from $0.6 \pm 0.1\%$ to $2.2 \pm 0.6\%$ for Higgs masses ranging from 70 GeV/$c^2$ to 140 GeV/$c^2$.

The shape of the observed $b$-tagged dijet invariant mass distribution is fit, using a binned maximum-likelihood method, to a combination of signal, fake double-tag events, and QCD, $t\bar{t}$ and $Z$ + jets backgrounds. The QCD and signal normalizations are left free in the fit while the normalizations of the $t\bar{t}$, $Z$ + jets and fakes are constrained by Gaussian functions

to their expected values and uncertainties. The expected number of events ($\mu$) in each mass bin is:

$$\mu = f_{t\bar{t}} \cdot N_{t\bar{t}} + f_{Zjj} \cdot N_{Zjj} + f_{fakes} \cdot N_{fakes}$$
$$+ f_{QCD} \cdot N_{QCD} + f_{VH^0} \cdot (\varepsilon \cdot \mathcal{L} \cdot \sigma_{VH^0} \cdot \beta),$$

where $f_{t\bar{t}}$, $f_{Zjj}$, $f_{fakes}$, $f_{QCD}$, and $f_{VH^0}$ are the expected fractions of events in this given bin, and $N_{t\bar{t}}$, $N_{Zjj}$, $N_{fakes}$, and $N_{QCD}$ are, respectively, the total expected number of $t\bar{t}$, $Z$+jets, fake, and QCD events. The quantities $\varepsilon$, $\mathcal{L}$, and $\sigma_{VH^0} \cdot \beta$ represent the detection efficiency, integrated luminosity, and unknown $VH^0$ production cross section times branching ratio of $H^0$ decaying into $b\bar{b}$. The likelihood is:

$$L = G(N_{t\bar{t}}; \bar{N}_{t\bar{t}}, \sigma_{t\bar{t}}) \cdot G(N_{Zjj}; \bar{N}_{Zjj}, \sigma_{Zjj})$$
$$\cdot G(N_{fakes}; \bar{N}_{fakes}, \sigma_{fakes}) \cdot T$$

where $T = \prod_i P(n_i, \mu_i)$ and $P(n_i, \mu_i)$ is the Poisson probability for $n_i$ observed events with expected mean $\mu_i$ in bin $i$. $G(x; \bar{x}, \sigma)$ is Gaussian in $x$, with mean $\bar{x}$ and width $\sigma$.

The fit yields $\sigma_{VH^0} \cdot \beta = 44 \pm 42$ pb for $M_{H^0} = 70$ GeV/$c^2$, statistically compatible with zero signal. For larger masses, zero signal contribution is preferred. Table I shows the result of the fits as a function of the Higgs mass. Figure 2 shows the $b$-tagged dijet invariant mass distribution for the data compared to the results of the fit for $M_{H^0} \geq 80$ GeV/$c^2$.

Since the observed distribution is consistent with standard model background expectations, we place limits on $p\bar{p} \to VH^0$ production. Systematic uncertainties on the 95% C.L. limits were determined by varying each source of error by $\pm 1\sigma$. The separate contributions arise from luminosity, jet energy scale, double $b$-tagging efficiencies, QCD radiation, limited Monte Carlo statistics, and background normalizations and shapes. The total systematic uncertainty is in the range $26\% - 30\%$. The 95% C.L. limits are summarized in Table I and Figure 3. The resulting bounds fall rapidly from 117 pb at $M_{H^0} = 70$ GeV/$c^2$ to values between 15 and 20 pb for $M_{H^0} > 105$ GeV/$c^2$.

To combine our results with the ones from [6], the leptonic analysis was first extended up to $M_{H^0} = 140$ GeV/$c^2$. From the 95% C.L. limits on $\sigma(p\bar{p} \to WH^0)$, the corresponding limits on $VH^0$ production were calculated. We used the program PYTHIA to compute the standard model prediction for the ratio $\sigma(ZH^0)/\sigma(WH^0)$. The leptonic analysis efficiency for $ZH^0$ events relative to that for $WH^0$ events was estimated to be $(10 \pm 2)\%$. The data from both channels were then fitted simultaneously. Correlations between systematic uncertainties due to luminosity, QCD radiation, and $b$-tagging efficiency were taken into account. All other systematic uncertainties were considered uncorrelated. The 95% C.L. limits range from 16 to 24 pb and are shown in Table I and Figure 3.

The sensitivity of the present search is limited by statistics to a cross section approximately two orders of magnitude larger than the predicted cross section for standard model Higgs production [5]. It should be noted that, because these limits were derived from a shape fit, they only apply to a very restricted region of parameter space in the minimal supersymmetric extension of the standard model. For the next Tevatron run we hope for an approximately twenty-fold increase in the total integrated luminosity, a factor of two improvement in the double $b$-tagging efficiency, and we plan to install a more efficient, dedicated Higgs trigger. The limit is expected to decrease by about an order of magnitude.

We thank the Fermilab staff and the technical staffs of the participating institutions for their vital contributions. This work was supported by the U.S. Department of Energy and National Science Foundation; the Italian Istituto Nazionale di Fisica Nucleare; the Ministry of Education, Science and Culture of Japan; the Natural Sciences and Engineering Research Council of Canada; the National Science Council of the Republic of China; the Swiss National Science Foundation; and the A. P. Sloan Foundation.

# REFERENCES


[1] P.W. Higgs, Phys. Lett. **12**, 132 (1964), Phys. Rev. Lett. **13**, 508 (1964), Phys. Rev. **145**, 1156 (1966); F. Englert and R. Brout, Phys. Rev. Lett. **13**, 321 (1964).

[2] R. Barate *et al.*, Phys. Lett. **B 412** 425 (1997); P. Abreu *et al.*, Eur. Phys. J. **C2** 1 (1998); M. Acciarri *et al.*, Phys. Lett. **B 411** 373 (1997); K. Ackerstaff *et al.*, Eur. Phys. J. **C1** 425 (1998); The LEP working group for Higgs boson searches, Report No. CERN-EP-98-046, 1998.

[3] The LEP Electroweak Working Group and the SLD Heavy Flavours and Electroweak Groups, Internal Report No. LEPEWWG-98-01, 1998.

[4] M. Carena *et al.*, Nucl. Phys. **B 461** 407 (1996); H. E. Haber *et al.*, Z. Phys. **C75** 539 (1997).

[5] S.L. Glashow, D.V. Nanopoulos and A. Yildiz, Phys. Rev. D **18**, 1724 (1978); A. Stange, W. Marciano and S. Willenbrock, Phys. Rev. D **49**, 1354 (1994); Phys. Rev. D **50**, 4491 (1994).

[6] F. Abe *et al.*, Phys. Rev. Lett. **79**, 3819 (1997).

[7] S. Abachi *et al.*. Report No. Fermilab-Conf-96-258-E, 1996.

[8] F. Abe *et al.*, Nucl. Instrum. Methods Phys. Res., Sect. A **271**, 387 (1988).

[9] D. Amidei *et al.*, Nucl. Instrum. Methods Phys. Res., Sect. A **350**, 73 (1994).

[10] In the CDF coordinate system, $\phi$ and $\theta$ are the azimuthal and polar angles with respect to the proton beam direction. The pseudorapidity $\eta$ is defined as $-\ln[\tan(\theta/2)]$. The transverse momentum of a particle is $p_T = p\sin\theta$. The analogous quantity using calorimeter energies is called the transverse energy $E_T$. The difference between the vector sum of all the transverse energies and zero is the missing transverse energy $\not\!\!E_T$.

[11] F. Abe *et al.*, Phys. Rev. D **45**, 1448 (1992).

[12] F. Abe *et al.*, Phys. Rev. Lett. **74**, 2626 (1995).

[13] T. Sjöstrand, Comput. Phys. Commun. **82**, 74 (1994).

[14] R. Vilar, Ph. D. thesis, Universidad de Cantabria, unpublished, 1998.

[15] F. Abe *et al.*, Phys. Rev. Lett. **80**, 2773 (1998).

[16] G. Marchesini *et al.*, Comput. Phys. Commun. **67**, 465 (1992).

[17] F. Abe *et al.*, Phys. Rev. Lett. **79**, 1992 (1997).

[18] R. M. Barnett *et al.*, Phys. Rev. D **54**, 1 (1996).

[19] P. Avery *et al.*, Cornell Report No. CSN-212, 1985.

## TABLES

TABLE I. Summary of the hadronic analysis fit results, standard model predictions for $\beta\sigma$, and 95% C.L. limits from the hadronic, leptonic, and combined analyses.

| $M_{H^0}$ (GeV/$c^2$) | $\beta\sigma$ (pb) fit | $\beta\sigma$ (pb) SM | $\beta\sigma$ (pb) had. limit | $\beta\sigma$ (pb) lep. limit | $\beta\sigma$ (pb) comb. limit |
|---|---|---|---|---|---|
| 70 | $44 \pm 42$ | 1.13 | 117.3 | 21.9 | 23.1 |
| 80 | $0^{+25}_{-0}$ | 0.76 | 53.2 | 28.2 | 23.8 |
| 90 | $0.0^{+5.4}_{-0.0}$ | 0.55 | 28.9 | 29.0 | 18.0 |
| 100 | $0.0^{+4.2}_{-0.0}$ | 0.41 | 22.8 | 27.2 | 16.8 |
| 110 | $0.0^{+3.6}_{-0.0}$ | 0.30 | 18.7 | 30.1 | 17.1 |
| 120 | $0.0^{+3.7}_{-0.0}$ | 0.20 | 17.6 | 25.0 | 16.0 |
| 130 | $0.0^{+3.5}_{-0.0}$ | 0.12 | 16.7 | 38.5 | 19.7 |
| 140 | $0.0^{+3.8}_{-0.0}$ | 0.06 | 15.3 | 34.5 | 17.2 |

FIGURES

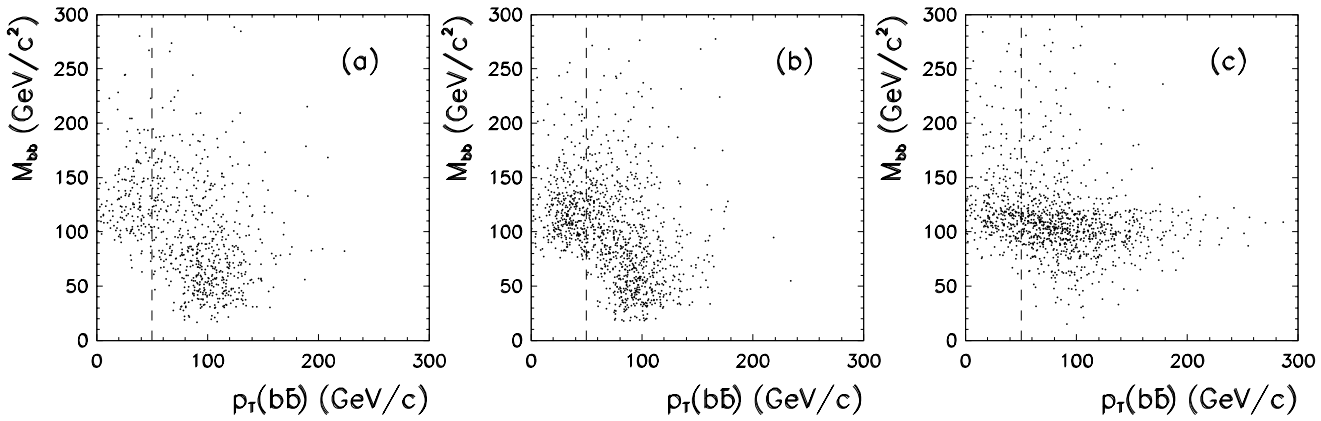


FIG. 1. $M_{b\bar{b}}$ vs $p_T(b\bar{b})$ for (a) selected sample, (b) $b\bar{b}/c\bar{c}$ Monte Carlo and (c) $W/Z + H^0$, $M_{H^0} = 100$ GeV/$c^2$. The vertical dashed lines indicate the $p_T(b\bar{b}) \geq 50$ GeV/$c$ cut.

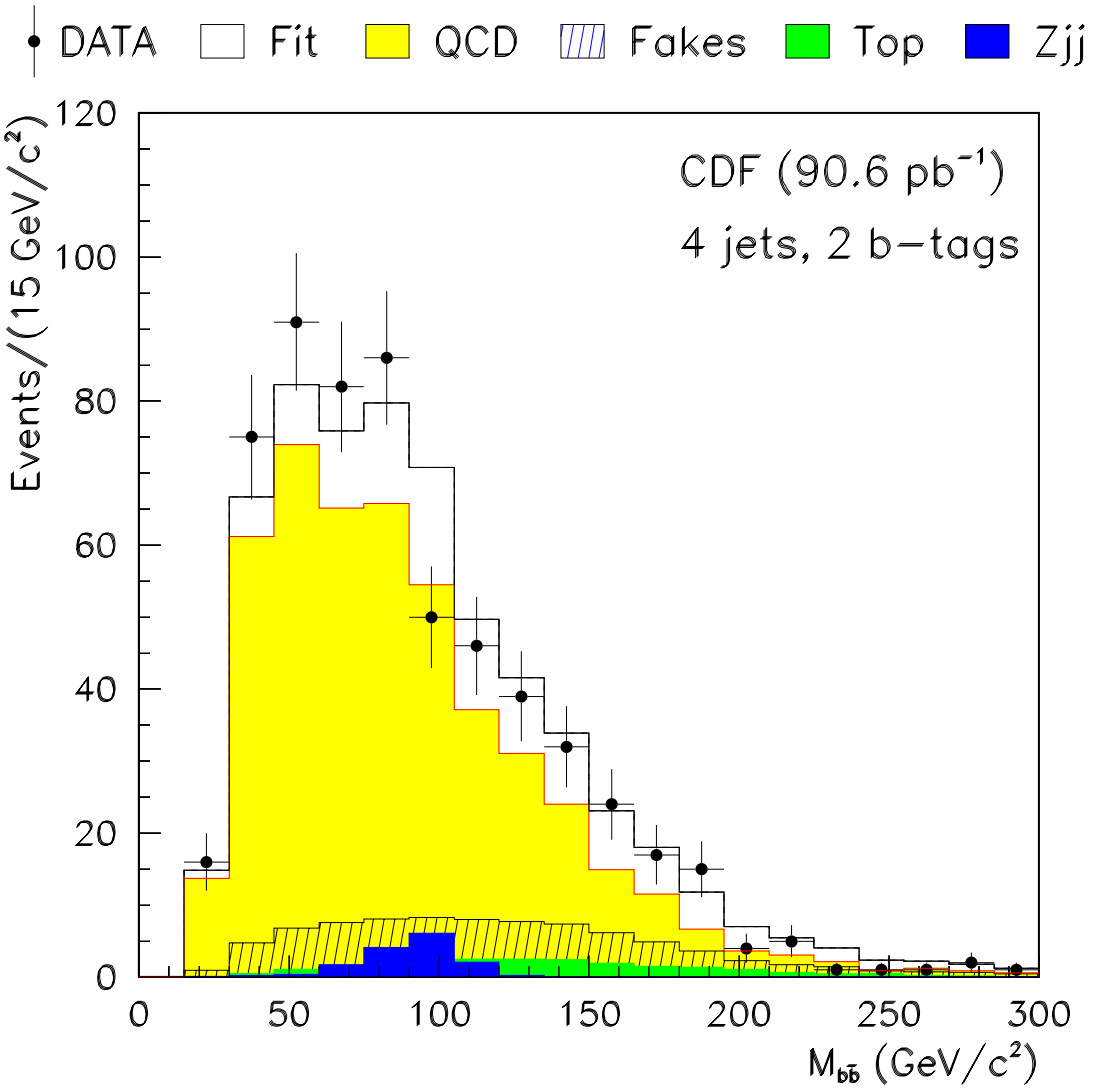


FIG. 2. Invariant mass distribution, $M_{b\bar{b}}$, for 90.6 pb$^{-1}$ of CDF data (points) compared to the fit prediction. The solid line is the sum of the QCD, fakes, $t\bar{t}$, and $Z$ + jets components.

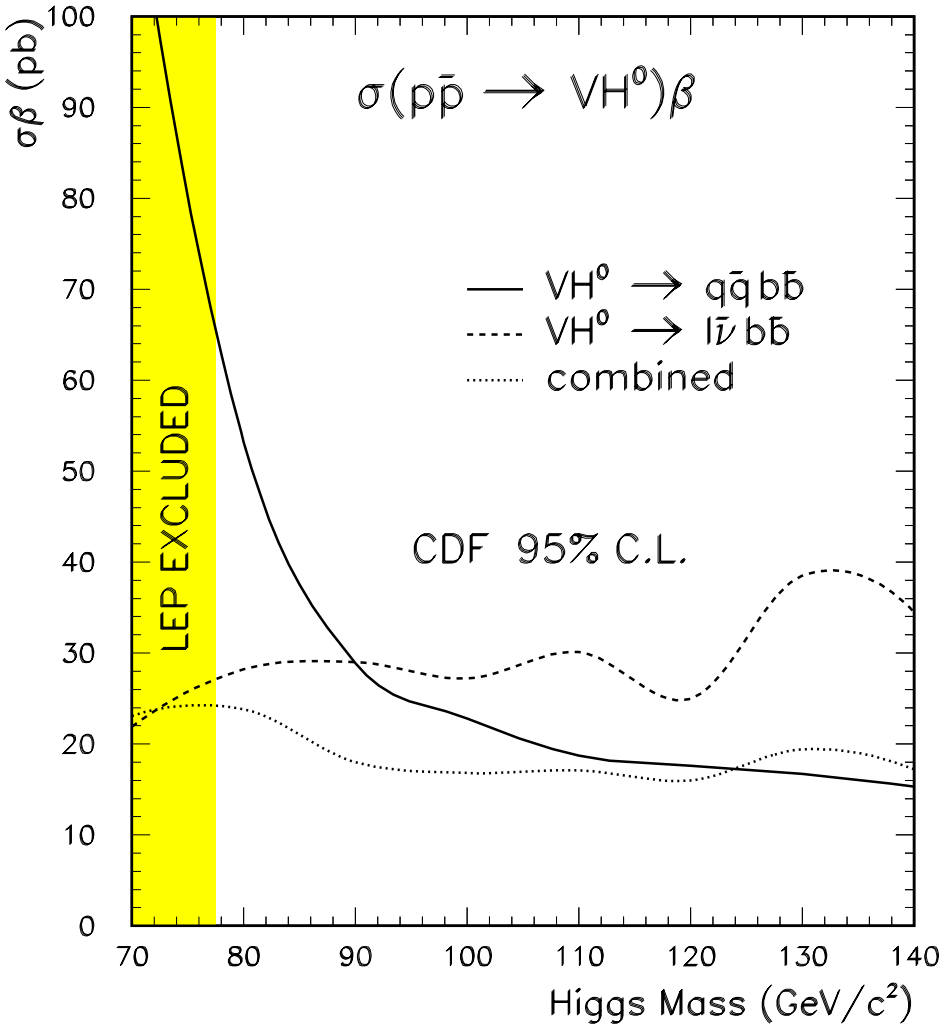


FIG. 3. The CDF 95% C.L. upper limits on $\sigma(p\bar{p} \to VH^0) \cdot \beta$ where $\beta = \mathcal{B}(H^0 \to b\bar{b})$. The mass region excluded by the LEP experiments for a standard model Higgs is also shown.